



## Magnetostratigraphy of the Miocene Las Arcas Formation, Santa María Valley, northwestern Argentina

Cecilia M. Spagnuolo <sup>a,\*</sup>, Sergio M. Georgieff <sup>a</sup>, Augusto E. Rapalini <sup>b</sup>

<sup>a</sup> CONICET, IESGLO, Instituto de Sedimentología, Facultad de Ciencias Naturales y Fundación Miguel Lillo, Universidad Nacional de Tucumán, Miguel Lillo 205-251, T4000JFE, San Miguel de Tucumán, Argentina

<sup>b</sup> IGEBa, CONICET-Depto. Cs. Geológicas, FCEyN, Univ. Buenos Aires, Pabellón 2, Ciudad Universitaria, C1428EHA, Buenos Aires, Argentina



### ARTICLE INFO

#### Article history:

Received 14 January 2015

Received in revised form

29 June 2015

Accepted 3 July 2015

Available online 8 July 2015

#### Keywords:

Magnetostratigraphy

Paleomagnetism

Miocene

Northwestern Argentina

Las Arcas Formation

Sedimentation rate

### ABSTRACT

The first magnetostratigraphic study of the Las Arcas Formation (Late Miocene) was carried out in Las Totoritas creek ( $26^{\circ}12'S$ ;  $65^{\circ}47'W$ , NW Argentina), a key place in between of two geological provinces: Northwestern Pampean Ranges and Eastern Cordillera, in northwestern Argentina. This was accompanied by isotopic dating ( $9.01 \pm 0.12$  Ma,  $^{40}\text{Ar}$ – $^{39}\text{Ar}$  in amphibole) of the unit, obtained from a 3.4 m thick tuff intercalated at ~45 m above the base. The Las Arcas Formation is 810 m thick at the sampling locality and it is mainly composed of tabular reddish conglomerates, sandstones and siltstones in both coarsening- and thickening-upward arrangements. The exposed section was sampled at 48 sites, 26 of which are interpreted as carrying primary magnetization. The new magnetostratigraphic column was correlated with the Geomagnetic Polarity Time Scale (GPTS), and suggests that deposition of the Las Arcas Formation strata started at around 9.1 Ma and ended around 6.8 Ma. The paleomagnetic pole obtained for this unit ( $\text{Dec} = 8.7^{\circ}$   $\text{Inc} = -43.9^{\circ}$   $\text{dp} = 14.9$  dm 9.3) indicates that this area underwent non-significant rotation ( $11.0^{\circ} \pm 13.6^{\circ}$ ) since the Late Miocene.

© 2015 Elsevier Ltd. All rights reserved.

## 1. Introduction

Since Matuyama (1929) found paleo-directions of Earth's magnetic field in volcanic rocks from Japan and North China corresponding to normal and reverse polarities, numerous magnetostratigraphic studies have been carried out around the world for stratigraphic correlations and relative geochronological studies (e.g. Opdyke and Channell, 1996), especially in Cenozoic sedimentary foreland successions (e.g. Johnson et al., 1986; Reynolds et al., 1990; Homke et al., 2004; Sun et al., 2005), due to the high Cenozoic reversal frequency and the high sedimentation rates of these deposits. Successful magnetostratigraphic studies permit assigning a quasi-continuous age to sedimentary successions by correlating the local magnetostratigraphic column with the Global Polarity Time Scale (GPTS, Cande and Kent, 1995; Huestis and Acton, 1997; Gradstein et al., 2004, 2012). The southern Central Andes are characterized by a complex magmatic and tectosedimentary evolution (e.g. Jordan et al., 1993; Marrett and Strecker,

2000; Kay and Mpodozis, 2002; among others). Numerous magnetostratigraphic studies in Neogene Andean foreland successions have been published in the last two decades (e.g. Johnson et al., 1986; Reynolds et al., 1990, 2001; Jordan et al., 1990; Malizia et al., 1995; Irigoyen et al., 2000; Ré, 2008; Zambrano et al., 2010; Galli et al., 2014).

Many authors postulate a Cenozoic tectonic rotation pattern in NW Argentina (Aubry et al., 1996; Taylor et al., 2005; Arriagada et al., 2006). When the data are analyzed in detail, the pattern is not continuous (Aubry et al., 1996; Spagnuolo et al., 2008; Zambrano et al., 2010; Japas and Ré, 2012) nor it is related to a large scale rigid body rotation (oroclinal bending) but to local block rotations associated to displacements along major oblique lineaments, such as the Tucumán and El Brete Lineaments (Mon, 1979). Some authors suggested that the rotations found in NW Argentina are controlled by two large lineaments (Tucumán Lineament and Valle Fértil Fault Zone) and smaller parallel lineaments (Vizán et al., 2013) in a fractal model (Ré et al., 2001). At around  $27^{\circ}$  S the subduction angle of the Nazca Plate beneath South America changes from normal ( $\sim 30^{\circ}$ ) in the north to subhorizontal in the south. Associated with it, a major physiographic change occurs at the transition between the Puna and the Pampean Ranges. Also in that

\* Corresponding author.

E-mail address: [cecispagnuolo@yahoo.com.ar](mailto:cecispagnuolo@yahoo.com.ar) (C.M. Spagnuolo).

region lineaments oblique to the Andean chain are notorious (Fig. 1). The Tucumán Lineament has been called Tucumán Transfer Zone (TTZ; de Urreiztieta et al., 1996; Coutand et al., 2001) being a dextral transpressive zone of SW–NE strike (Mon, 1976, 1979; de Urreiztieta et al., 1996; Coutand et al., 2001). Correlation between the topography of the basins and ranges with the regional pattern of thrust faults characterizes the region (de Urreiztieta et al., 1996). To the north of 27° S, the basins and ranges are elongated into a NNE direction (Laguna Blanca and Quilmes Ranges) while to the south of the 27°30'S they are NW trending (Velasco, Ambato-Ancasti Ranges). In the transition zone (TTZ) the trends are approximately NE (Hualfín-Las Cuevas, El Durazno, Nevados de Aconquija, Belén), suggesting possible tectonic rotations associated

with these lineaments (Vizán et al., 2013). Their influence however, in the kinematic and tectonic evolution of the Andean Orogen and in the Neogene basins is far from being well understood. New paleomagnetic data from Cenozoic sedimentary strata in this region may help in constraining the kinematic evolution of the Andean foreland at these latitudes.

The Santa María-Hualfín Basin (Fig. 1) originated with extension and active faulting from the Paleogene until 4.8 Ma when regional compression began (Bossi and Muruaga, 2009). Ages from apatite fission tracks (Sobel and Strecker, 2003) suggest a 6 Ma uplift of the Aconquija, Quilmes and Cumbres Calchaquíes Ranges, which arose as deformation migrated to the south (Mortimer et al., 2007). Strecker (1987) defined the beginning of the compressive phase

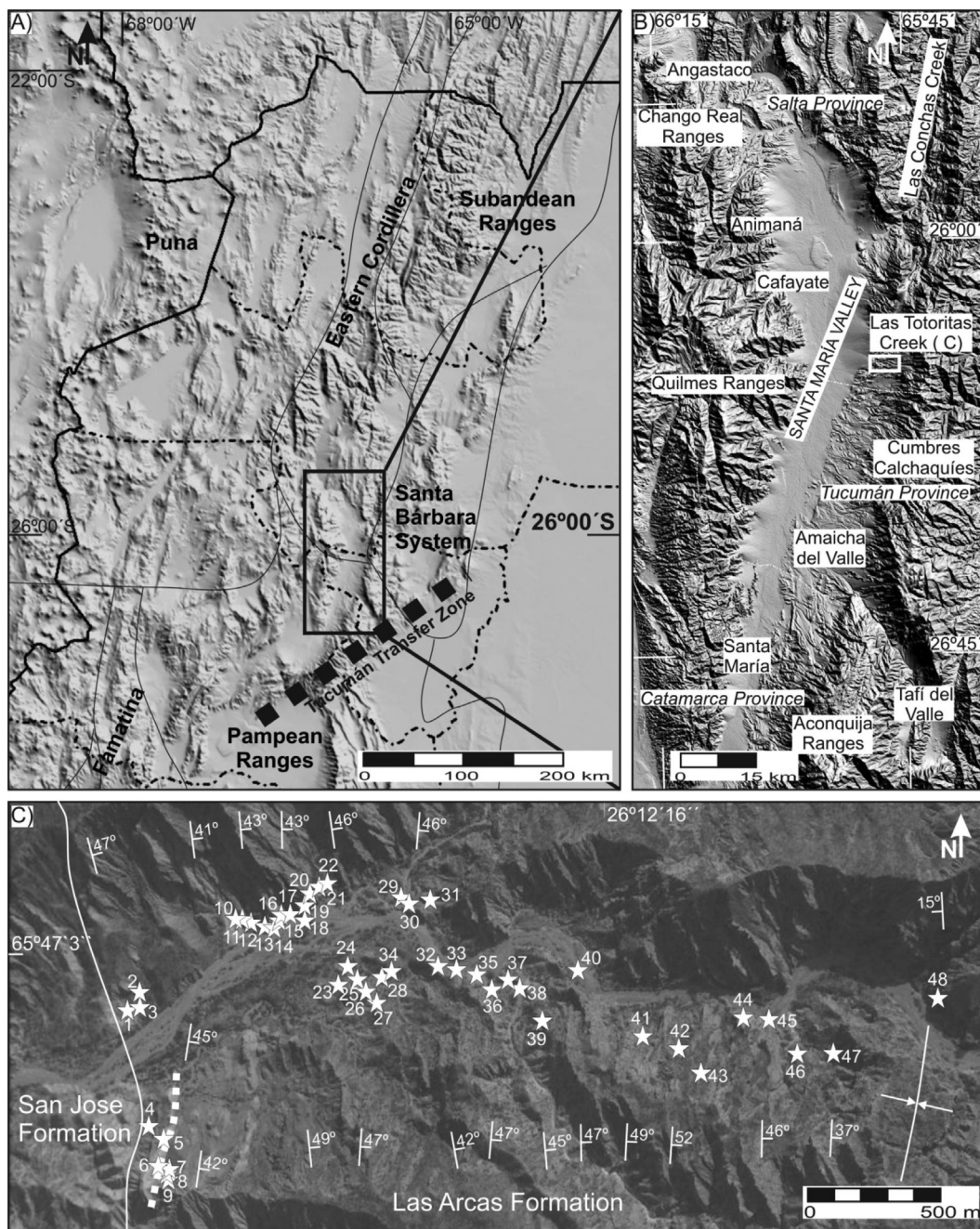


**Fig. 1.** A) Digital elevation model (DEM) of NW Argentina. B) DEM of the Santa María Valley with the location of the sampling area (Las Totoritas creek). C) Aerial photograph of the Las Totoritas creek with the paleomagnetic sites and geological information. Full line: contact between formations. Dotted line: tuff outcrops.

after 5.2 Ma, and Georgieff (1996, 1998) related this event with the development of the intra Andalhuala unconformity in southern Santa María Valley. Bossi et al. (2001) divided the Cenozoic deposits into five allostratigraphic units: I prerift (Saladillo and Yacomisqui Formations), IIa initial rift stage (San José, Las Arcas and Chiquimil B Formations), IIb rift climax stage (Chiquimil A, lower part of the Andalhuala Formation), III initial compressive stage (upper part of Andalhuala and Corral Quemado Formations) and IV climax compressive stage (Yasyamayo Formation).

A magnetostratigraphic study was conducted in the Las Arcas Formation (LAF) exposed along Las Totoritas creek ( $26^{\circ} 12'S$ ;  $65^{\circ} 47'W$ ), a Santa María River tributary on the eastern slope of the Cumbres Calchaquíes Ranges in southern Salta province (Fig. 1). The LAF (Galván and Ruiz Huidobro, 1965) belongs to the Santa María Group (Ruiz Huidobro, 1960; Galván and Ruiz Huidobro, 1965; Bossi et al., 2001). It is composed mainly of red fine sandstones and mudstones. Its exposures extend over more than  $15,000 \text{ km}^2$ . The magnetostratigraphic study was accompanied by an isotopic dating for this unit, obtained from an intercalated tuff at ~45 m above the base. The correlation of the 810 m local magnetostratigraphic column with the GPTS permits age and accumulation rate constraints for the LAF, while the paleomagnetic pole obtained suggests very minor to no tectonic rotation in the area. This is the first magnetostratigraphic study on this unit although the paleomagnetic study published by Aubry et al. (1996) in red sediments in the southern Santa María Basin might belong to the LAF.

## 2. Geologic setting and stratigraphy

The Santa María Valley is a morphotectonic feature that comprises SE Salta, W Tucumán and NE Catamarca provinces in NW Argentina. It is bordered on the east by the Aconquija and the Cumbres Calchaquíes Ranges and on the west by the Quilmes Ranges (Fig. 1b). This region is part of the Pampean Ranges (*Sierras Pampeanas*) tectonic province, which is composed of N–S oriented mountain blocks with dominant Precambrian to Early Cambrian basement outcrops uplifted by west-dipping reverse faults in the Late Cenozoic (González Bonorino, 1950; Ramos, 1999).

The general stratigraphy of the LAF area begins with a Precambrian to Lower Cambrian metamorphic and igneous basement (Ruiz Huidobro, 1966; Toselli and Rossi, 1998; Toselli et al., 1999) covered by Cenozoic deposits. Those deposits are composed by the Paleogene Saladillo Formation (Peirano, 1956; Galván and Ruiz Huidobro, 1965; Bossi et al., 2001) and the Neogene Santa María Group (Ruiz Huidobro, 1960; Galván and Ruiz Huidobro, 1965; Bossi and Palma, 1982). The latter was subdivided into the San José, Las Arcas, Chiquimil, Andalhuala and Corral Quemado Formations overlain by the Yasyamayo Formation and Quaternary sedimentary deposits.

The base of the Saladillo Formation exhibits fine lacustrine facies with a basal breccia that passes to red fluvial sandstones (Bossi et al., 1998). The San José Formation (Galván and Ruiz Huidobro, 1965) overlies the Saladillo Formation and is characterized by green-yellowish pelites and marls with interbedded limestones of a lacustrine setting. The Las Arcas Formation (Galván and Ruiz Huidobro, 1965) consists of fine red sandstones and siltstones intercalated with some lenses of conglomerate typical of a fluvial setting (Bossi and Palma, 1982) and was dated in  $6.88 \pm 0.06 \text{ Ma}$  (Jujuí creek,  $^{40}\text{Ar}$ – $^{39}\text{Ar}$ , Georgieff and Díaz, 2014). The Chiquimil Formation changes its sedimentary setting from south to north (Ibañez, 2001): fluvial strata in the south (Catamarca Province), lacustrine facies in the center (Tucumán Province) and a sabkha or hypersaline lake setting in the north (Salta Province). The Chiquimil Formation was dated in  $6.68 \pm 0.02 \text{ Ma}$  (Corral Quemado locality, K–Ar method, Marshall et al., 1979),  $7.14 \pm 0.02 \text{ Ma}$  (Corral

Quemado locality,  $^{40}\text{Ar}$ – $^{39}\text{Ar}$ , Latorre et al., 1997) and  $6.70 \pm 0.05 \text{ Ma}$  (Corral Quemado locality, K–Ar, Butler et al., 1984). The Andalhuala Formation is composed of sandy and conglomeratic fluvial packages with abundant fossils (Marshall and Patterson, 1981). It was dated in  $6.02 \pm 0.04 \text{ Ma}$  (Chiquimil/Entre Ríos locality) and  $7.3 \pm 0.1 \text{ Ma}$  (Corral Quemado locality) (both with K–Ar method, Marshall et al., 1979),  $5.22 \text{ Ma}$  (Chiquimil locality, K–Ar, without quoting errors, Strecker, 1987). The Corral Quemado Formation consists of conglomeratic facies with metamorphic clasts, while the Yasyamayo Formation is composed of conglomerates with volcanic clasts and intercalated red sandstones and mudstones.

## 3. Isotopic dating

To correlate the local magnetostratigraphic column with the GPTS, an  $^{40}\text{Ar}$ – $^{39}\text{Ar}$  date was obtained at SERNAGEOMIN laboratories (Servicio Nacional de Geología y Minería, Chile). Amphibole crystals were separated from a 3.40 m tuff (Fig. 2) intercalated ~45 m above the base of the LAF between paleomagnetic sites 5 and 6. Fig. 3 and Appendix 1 show stepwise degassing results from the sample. A plateau age of  $9.01 \pm 0.12 \text{ Ma}$  was calculated with a MSWD = 0.64. The integrated age ( $9.56 \pm 0.17 \text{ Ma}$ ) is similar to the plateau age. The isochron analyses yields an age of  $8.79 \pm 0.14 \text{ Ma}$  with a MSWD error of 0.35 ( $2\sigma$ ).

## 4. Paleomagnetic sampling

Along Las Totoritas creek (Fig. 1), the LAF has a transitional contact with the underlying San José Formation (Fig. 2) and is characterized by the presence of grayish orange pink (10R 7/2, Rock Color Chart) massive and laminated siltstones with intercalated conglomeratic sandstones. In some cases, they exhibit conglomeratic lenses and heterolithic stratification with fibrous-gypsum veins (Fig. 4). Four intercalated beds of green and gray mudstones are exposed between 2 and 9 m and correspond to lacustrine facies. Some molds of *Neocorbicula* sp. were found in the siltstones. Around 350 m above the base both color and grain size change, with the strata becoming coarser and a pale yellowish brown (10YR 6/2, Rock Color Chart). Tabular beds of medium to coarse, poorly-sorted sandstone, with intercalations of conglomeratic lenses and subordinate massive and parallel laminated siltstones, characterize the upper section. At the 810 m level, the strata become folded and thrusted. The top of the LAF is truncated by a high angle reverse fault which exhumes around 200 m of grayish fine sandstones and at least 250 m of reddish sedimentary breccias of the Andalhuala Formation.

At Quebrada del Mal Paso, few km to the south of Las Totoritas creek, Georgieff and Díaz (2014) identified four major sedimentary facies within the LAF, from base to top:

- Facies 1 (284.6 m): alternation of red siltstones and sandstones with green siltstones and claystones.
- Facies 2 (321.9 m): alternation of red brownish sandstones and siltstones and lenticular sandstones and pebble conglomerates composed by clasts of granites (70%), metamorphites (20%) and volcanites (10%).
- Facies 3 (339.4 m): 8–10 m thick sandstones bodies intercalated with thin tabular siltstones.
- Facies 4 (117.6 m): medium to coarse sandstones and coarse gravelly deposits.

The paleoenvironment is interpreted as coarsening- and thickening-upward fluvial deposits, meandering rivers at the base,

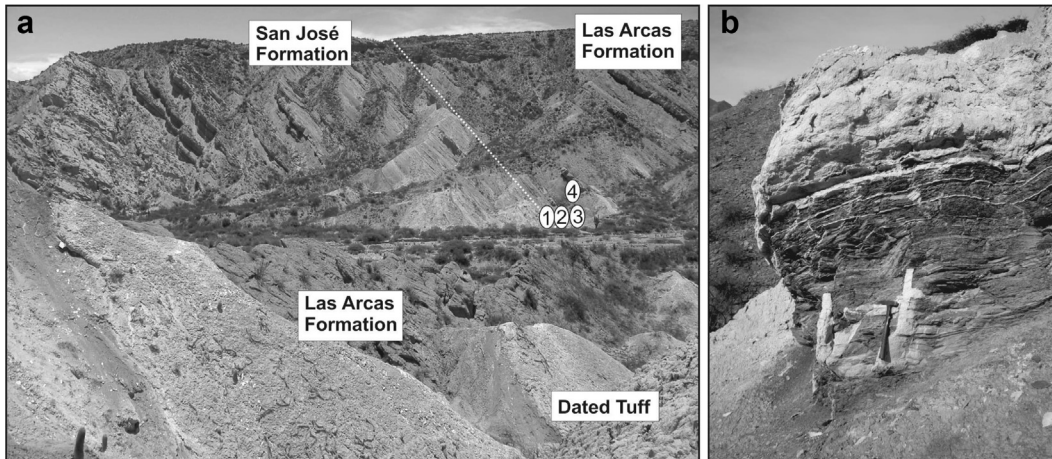


**Fig. 2.** a) Photograph of the San José and Las Arcas Formations with the dated tuff. The numbers indicate the paleomagnetic sites and the dotted white line the contact between formations. b) Detailed photograph of the tuff dated by  $^{40}\text{Ar}$ - $^{39}\text{Ar}$  method (geological hammer at the base).

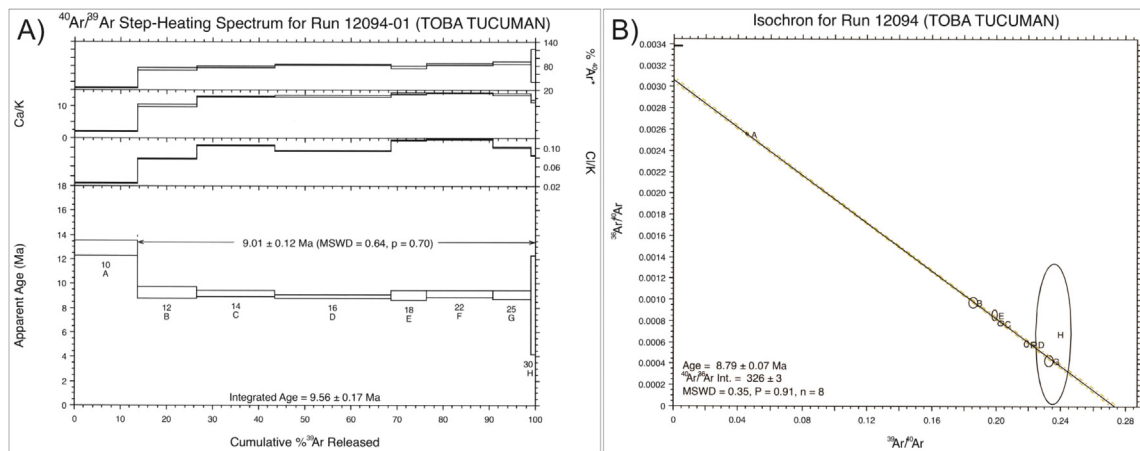


**Fig. 3.** A)  $^{40}\text{Ar}$ - $^{39}\text{Ar}$  step-heating spectrum for the tuff. B) Isochron. See the text for more details (Section 3).

which gradually passes into braided channels and transitionally became alluvial fans.

## 5. Laboratory procedures

One hundred and thirteen hand samples and twenty-six cores obtained with a portable battery-powered drill were collected from the LAF at forty-eight sites distributed along the Las Totoritas creek (Figs. 1 and 4). Samples were oriented by means of both sun and magnetic compasses in most cases. The sites were sampled with an average stratigraphic distance of ~10 m in the siltstones and ~20 m in the sandstones. In the laboratory, the hand samples were drilled and each core was sliced into one to four standard paleomagnetic specimens (2.2 cm height and 2.54 cm diameter).

In most cases, two specimens from each site were submitted to a pilot standard stepwise demagnetization procedure, one to thermal (95, 150, 190, 295, 350, 400, 450, 500, 530, 560, 580, 610, 630 and 650 °C) and one to AF demagnetization (3, 6, 9, 12, 15, 20, 25, 30, 35, 40, 50, 60, 70, 80, 90 and 100 mT) to evaluate the best demagnetization technique to be applied to the whole collection. Considering that the responses to the demagnetization procedure were not homogeneous in all sites, the remaining specimens were submitted to thermal (9 steps) or AF (14 steps) demagnetization or

a combination of both. Intensity and direction of the natural remanent magnetization were measured with a DC-SQUID (2G-750R) cryogenic magnetometer. AF cleaning was achieved by means of a static three-axes degausser attached to it. Thermal demagnetization was applied with an ASC dual chamber oven, with internal magnetic fields below 10 nT. Bulk magnetic susceptibility was measured with a Bartington MS-2 susceptibility meter after each thermal step to control possible chemical changes induced by heating of the samples. Magnetic components were determined by principal component analysis (Kirschvink, 1980) with maximum angular deviation (MAD) values generally under 15° (however, only 14% of the magnetic components were obtained with a MAD between 12° and 15° and just 3% of the magnetic components were obtained with a MAD>15°, Appendix 2).

Acquisition of isothermal remanence was performed with a pulse magnetizer (ASC Scientific IM.10-30) in order to characterize the magnetic carriers at each site. One sample per site was analyzed by submitting it at pulse direct magnetic fields of: 17, 29, 44, 61, 90, 150, 250, 350, 450, 600, 1000, 1310, 1640, 2300 and 2545 mT, and subsequent measurement of the isothermal remanence intensity after each step. After that, the sample was rotated 180° and back fields were applied with magnitudes of: 122, 137, 150, 250, 302, 350, 400, 450, 600 and 735 mT.

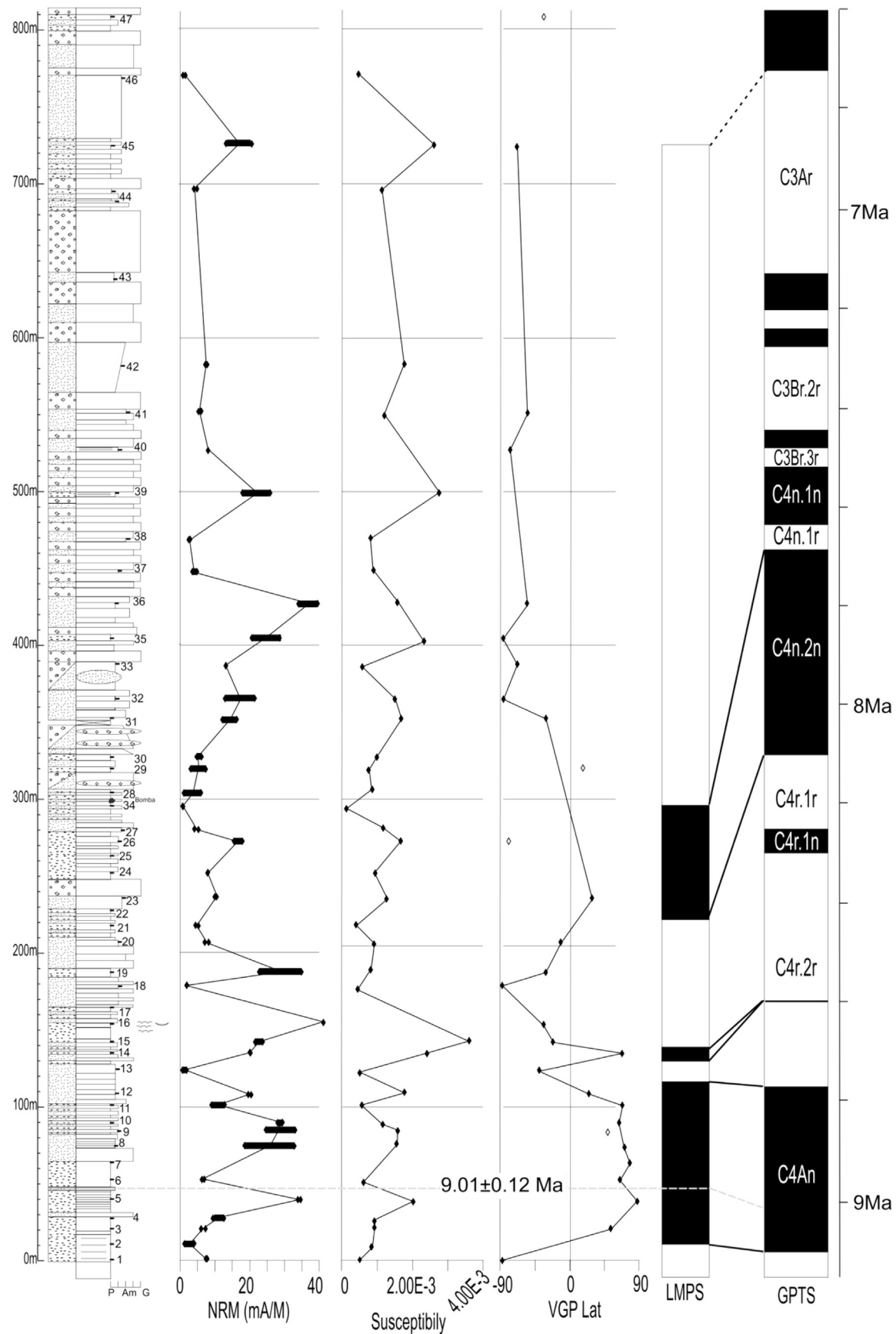


**Fig. 4.** Sedimentary log of the Las Arcas Formation that crops out in the Las Totoritas creek. Tuff position is indicated with a gray dashed line ( $9.01 \pm 0.12$  Ma), near the base of the profile. The numbers indicate the position of the paleomagnetic sites. NRM, bulk susceptibility and VGP latitude for each site are shown (open diamonds indicate sites not used for the magnetostratigraphic column). The obtained local magnetic polarity succession (LMPS) and its correlation with the GPTS (Gradstein et al., 2012) is also shown. See the text for more details (Sections 5, 6 and 7).

Low- and high-temperature thermomagnetic curves were performed for some specimens in an AGICO MFK1A-Kappabridge device.

## 6. Paleomagnetic results

Intensity of natural remanent magnetization varies between 0.6 and 295.5 mA/M and initial susceptibility between  $1.24 \cdot 10^{-4}$  and  $3.66 \cdot 10^{-3}$  SI (Fig. 4). IRM curves (Fig. 5) show a first partial saturation field below 150 mT and a second one over 2500 mT; while the back field curves show remanence coercivity between 40 and 350 mT, both suggesting that an antiferromagnetic plus a ferrimagnetic phase are present in the samples. Demagnetization curves (Fig. 6) are consistent with both magnetite and hematite as the magnetic carriers. The thermomagnetic curves are not reversible (Fig. 7). Heating curves reveal two transitions at 540–580 °C and 680 °C also suggesting the presence of magnetite and hematite as the main magnetic minerals in the LAF. In samples 18-2 and 28-3 a small step at -20 °C might suggest the presence of the Morin transition indicative of hematite.

In 20 sites a low temperature/alternating magnetic field (295–450 °C/6–60 mT) component (A) was isolated (Fig. 6;

Appendix 2a). An intermediate temperature and alternating magnetic field component (500–580 °C/30–100 mT) carried by Ti-magnetite (?) was isolated in 31 sites (Fig. 6; Appendix 2b; component B) and a high temperature component carried by hematite was isolated in 31 sites (Fig. 6; Appendix 2b; component C). These 3 components were also found by Aubry et al. (1996) in a paleomagnetic study of similar rocks to the south of our study area. In sites 4, 17, 22, 25, 28, 34, 38, 43 and 46 no magnetic components could be determined due to loss of samples, intrasite inconsistency of directions or unstable magnetic behavior during demagnetization.

Component A (Appendix 2a) likely corresponds to a viscous magnetization. The *in situ* direction ( $D = 1.0^\circ I = -37.5^\circ n = 26$  samples  $\alpha_{95} = 8.2^\circ$ ) is close to the present-day magnetic field at the sampling locality ( $D = -5.6^\circ I = -26.3^\circ$ ), and to the expected direction of the Earth Magnetic field dipole ( $D = 0^\circ, I = -44.5^\circ$ , Appendix 2a, Fig. 8a). The fold test (Watson and Enkin, 1993; Enkin, 2003) for this component is indeterminate because the data are too scattered and the structural correction is too small.

Components B and C have similar directions. In many sites both components could be isolated, however in some sites just one of

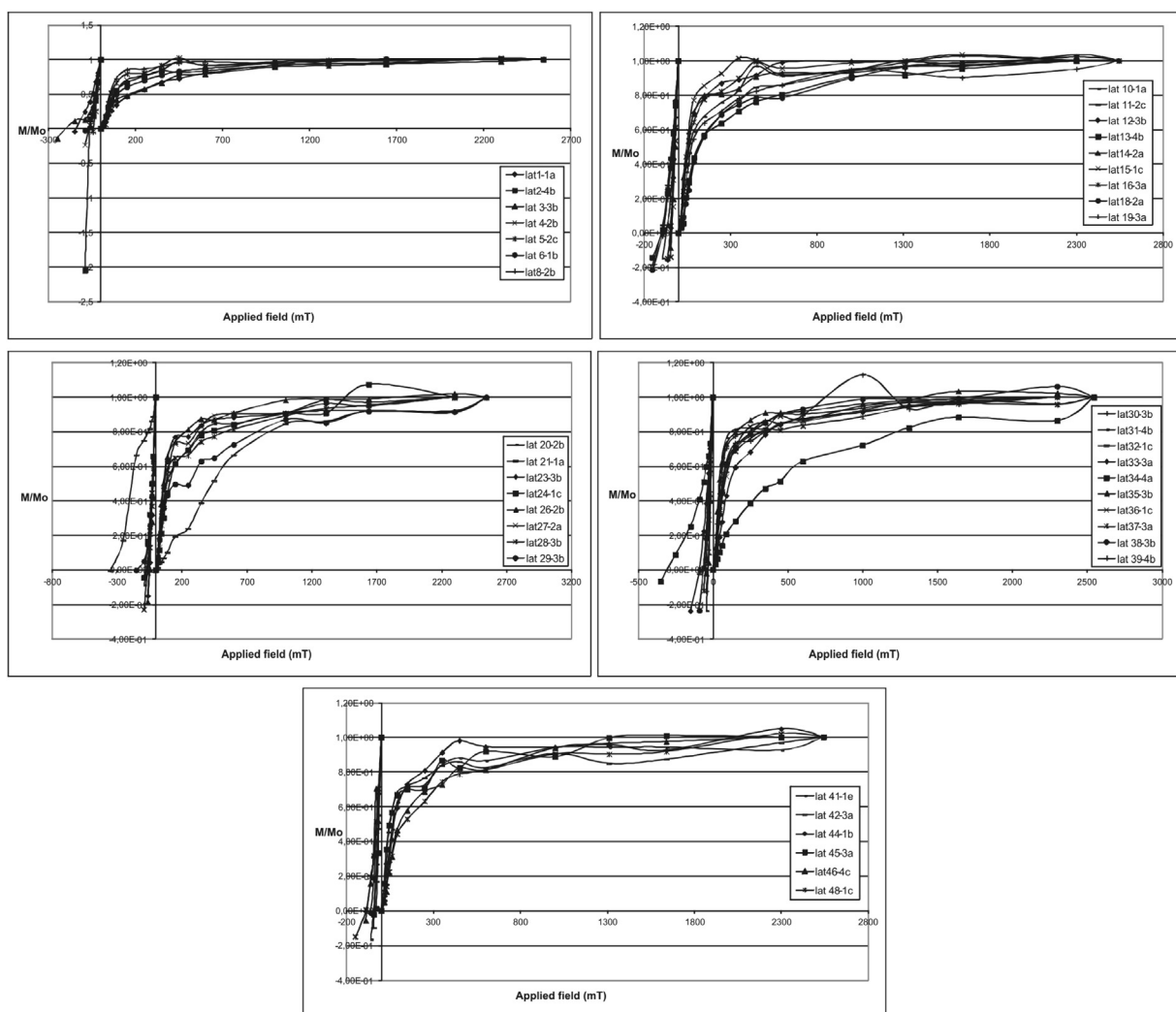


**Fig. 5.** Normalized isothermal remanent magnetization (IRM) and back field curves, indicating the presence of magnetite and hematite as magnetic carriers. More references in the text (Section 6).

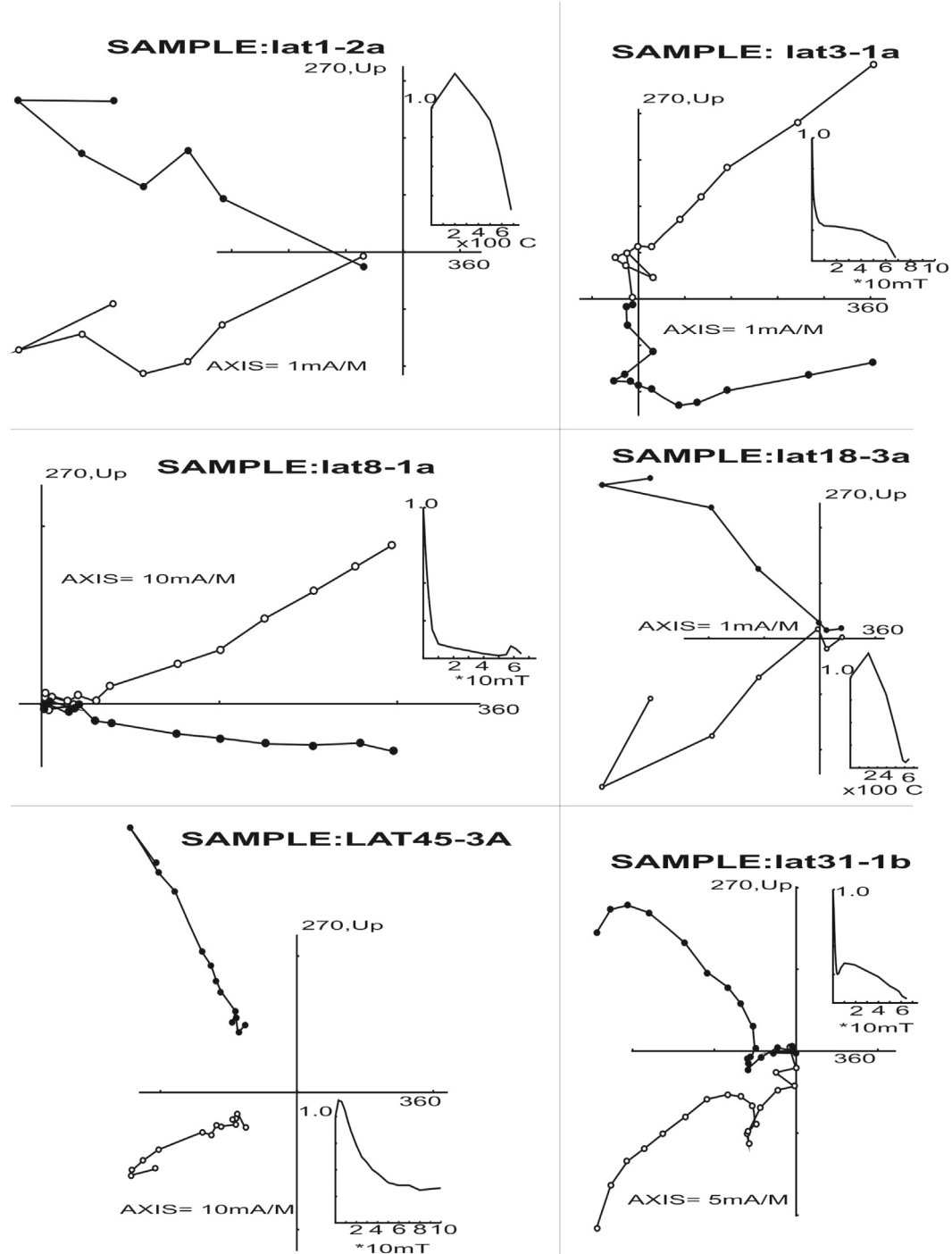


**Fig. 6.** Representative demagnetization behavior of analyzed specimens (geographic coordinates) of the Las Arcas Formation. In the vector diagram, closed (open) symbols represent projections in the horizontal (vertical) plane.

them was found. In samples where both components were found only one (that determined with higher precision) was considered (Appendix 3). Comparison of the mean site remanence directions before and after bedding correction does not show an important change in the statistical parameters because the sequence is almost homoclinal. This can be tested statistically by applying the fold test of Watson and Enkin (1993) (Fig. 9). After the application of the bedding correction the statistical parameters remain almost equal: kappa ( $K$ ) increases from 6.58 to 6.66 and  $\alpha_{95}$  diminishes from 12°

to 11.9°. Since 11 sites showed opposite polarities (Fig. 9a and b), a reversal test was applied. Both the negative inclination and the positive inclination mean directions show a discrepancy of just 6.4°. However the test of McFadden and McElhinny (1990) classifies the result as indeterminate due to a large critical angle (24.6°). The test of McFadden and Lowes (1981) indicates that groups of normal and reverse polarity share a common mean at 95% confidence. The occurrence of both polarities suggests that enough time elapsed during magnetization of the samples to average out secular

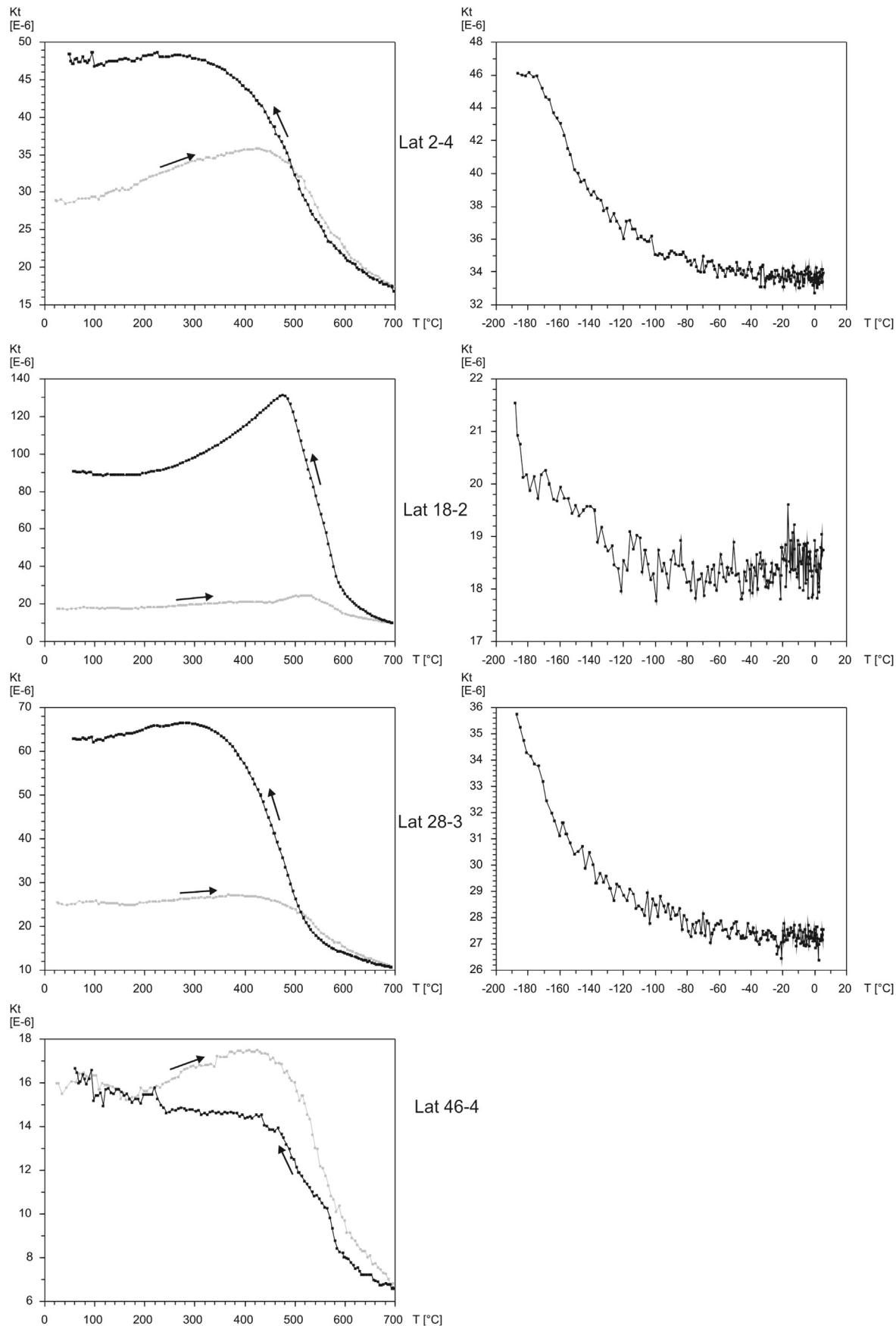


**Fig. 7.** Examples of thermomagnetic curves (bulk susceptibility versus temperature) for the Las Arcas Formation (after subtraction of paramagnetic susceptibility) at high temperatures (left column) and low temperatures (right column). The heating curves (gray line) show phases with Curie temperature of about 540–580 °C (Ti-magnetite) and 680 °C (hematite). The cooling curves (black line) show the samples are not reversible. In samples 18-2 and 28-3 a small step at –20 °C (Morin's transition) may suggest the presence of hematite.

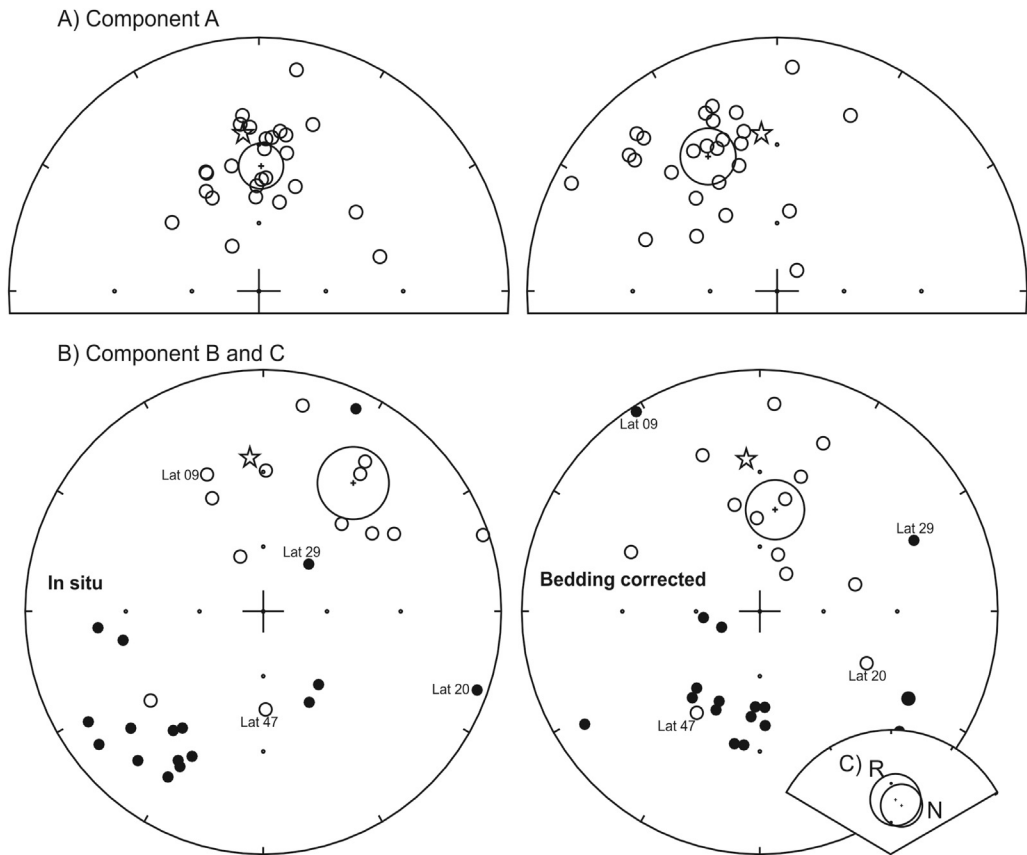


**Fig. 8.** In situ and bedded corrected distribution of sites remanence direction of the Las Arcas Formation. Equal angle stereoplot, open (closed) symbol corresponds to negative (positive) inclination. A) Component A. Star: present geomagnetic field. B) Component B and C. Lat 09, 20, 29 and 47 were not taken into account for constructing the magnetostratigraphic column nor for computing the pole position.

variation. A site-based average (without sites 9, 20, 29 and 47) of the bedding corrected remanence direction yields a mean direction at Dec = 8.7° Inc = −43.9° N (sites) = 26 α<sub>95</sub> = 11.9° (Fig. 8b). A paleomagnetic pole from these data was calculated for the LAF at 82.2°N, 22.4°E, dp = 14.9 dm = 9.3°. With the remanence polarity of each site a local magnetostratigraphic column was constructed (Fig. 4).

## 7. Interpretations and discussions

### 7.1. Tectonic rotation

The Andes show a change in its trend from NW–SE to N–S at approximately 18°S. This region is generally known as the “Bolivian Orocline” and comprises part of Bolivia, Perú and northern Chile

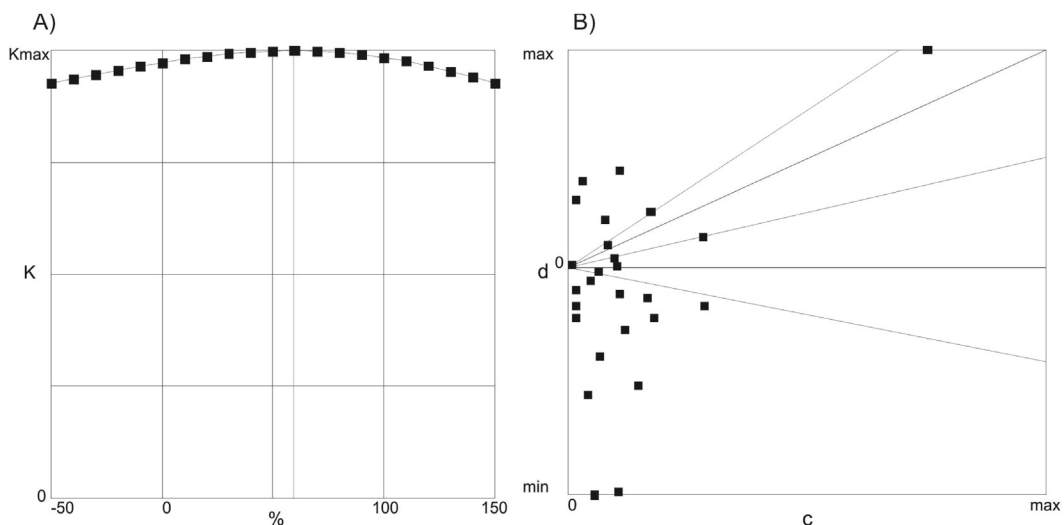


**Fig. 9.** Fold test of Watson and Enkin (1993) and tilt test of Enkin (2003). More references in the text (Section 6).

and Argentina. Paleomagnetic studies in the last three decades found systematic counterclockwise rotations to the north for the Bolivian Orocline, while towards the south clockwise rotations are the rule (e.g. Somoza et al., 1996; Beck, 1998; Randall, 1998; Arrigada et al., 2008). These rotations affect many Mesozoic and Cenozoic units along the South American margin. Since our sampling locality is within the region affected by the Central Andes rotation pattern (CARP; Somoza et al., 1996) the direction of the paleomagnetic pole of LAF (LAT: 82.2°N, 22.4°E) was compared with the expected direction for the 10 Ma reference pole of South America (Besse and Courtillot, 2002): 85.5°N 139.9°E A95 = 3.1° at the studied locality. A clockwise rotation of  $11.0^\circ \pm 13.6^\circ$  was obtained after using the algorithm proposed by Beck (1988) to compute the uncertainty. The values obtained indicate non-significant rotation of the study locality during the last 9 Ma. Lack of significant Andean tectonic rotations in this area reinforces previous ideas (Aubry et al., 1996; de Urreiztieta et al., 1996; Beck, 1998; Taylor et al., 1998; Coutand et al., 1999; Spagnuolo et al., 2010; Zambrano et al., 2010; Ré et al., 2001; Japas and Ré, 2006, 2012; Vizán et al., 2013) that rotations in this region do not follow a simple and uniform pattern. Beck (1998), Prezzi et al. (2004), Japas and Ré (2012) and Somoza and Tomlinson (2002) claim that no significant rotation should be expected in the region since 10 Ma. Therefore, older rotations in our study area cannot be excluded. Lack of rotation recorded coincides with the proposals of Japas and Ré (2012), and Domínguez et al. (2013). This area of the Santa María Valley would be explained due to particular tectonic characteristics as was pointed out by Ré et al. (2001); the northern part of the Santa María Valley belongs to a major tectonic block bordered by two regional lineaments, Pirquitas-Pozo Hondo and Cachi-Va. María (Ré et al., 2001), which shows vertical and strike-slip movements and no vertical axis block rotations (Sosa Gómez et al., 2014). According to this data, the study area is not tectonically linked with the Tucumán Transfer Zone (Mon, 1979; de Urreiztieta et al., 1996).

Comparison with the same expected direction also indicates a non-significant flattening of  $5.8^\circ \pm 9.9^\circ$ , suggesting minor if any significant compaction-induced anomaly in the remanence inclination.

## 7.2. Age of the unit and chronostratigraphic correlation

A magnetic polarity column of the LAF was obtained with results from 25 sites (Fig. 4). Site LAT 48 was not included because it was collected from a section affected by folding and thrusting and for which the proper stratigraphic position is ambiguous. In the lower section, most sites provide reliable polarity information while in the upper section, probably due to the increasing proportion of sandstones and gravels, fewer sites yielded useful results. The proposed correlation between magnetic polarity distribution of the LAF and the Global Polarity Time Scale (GPTS, Gradstein et al., 2012) is presented in Fig. 4. Using alternative GPTS (Huestis and Acton, 1997; Cande and Kent, 1995; Lourens et al., 2004) does not produce significant changes in the age of the sedimentary column.

In our sampled section, 6 geomagnetic field reversals were recorded defining 7 polarity zones. The  $^{40}\text{Ar}-^{39}\text{Ar}$  age of the dated tuff coincides with a normal polarity interval at the base of the section that coincides with the C4An subchron: 9.105–8.771 Ma (Gradstein et al., 2012). This is on top of a reversed interval that corresponds to the lower 20 m of the study section. The normal interval extends for ~100 m and is followed by a reversed interval of similar thickness. The presence of a short interval (determined by a single site) of normal polarity near its base can be explained as a recording of cryptochron C4r.2r-1 (Cande and Kent, 1992; Acton et al., 2006; Gradstein et al., 2012) with a duration of some 40 kyr

around 8.6 Ma. An alternative interpretation is that this short normal zone should be correlated with chron C4r.1n. The first alternative is chosen because of the stratigraphical position of the reversal and the interpretation of the accumulation rates (see Section 7.3).

The reversed interval is overlain by some 40 m of a normal interval that is correlated to the C4n.2n subchron. From around 270 m to the top at 730 m all sites show reverse polarity. The fact that in some cases stratigraphic thickness between correlative sites is from several tens to even one hundred meters make any correlation of the polarity recording of the upper section highly speculative. In any case, the exclusive reversed polarity suggests that the upper section was likely deposited within the C3Br–C3Ar chron, which extends from 7.528 to 6.733 Ma. The new dating of a tuff near the top of LAF at  $6.88 \pm 0.06$  Ma (Jujuil creek; Georgieff et al., 2014) reinforces this correlation. The short normal subchrons within this interval likely fall within the recording gaps. Based on this interpretation, deposition of the sampled section of the LAF must have started prior to 9.1 Ma and might have ended around 6.73 Ma.

The new  $^{40}\text{Ar}-^{39}\text{Ar}$  age for the LAF of  $9.01 \pm 0.12$  Ma, is younger than those previously proposed. Bossi and Muruaga (2009) suggested that the LAF was older than 12 Ma because it predated Farallón Negro volcanism. Halter et al. (2004) however, dated the Farallón Negro volcanism between 9.4 and 6.3 Ma. In Catamarca province, LAF was intruded and covered by andesitic volcanic rocks erupted at  $10.7 \pm 0.3$  Ma (Caelles et al., 1971). A dated tuff at the top of the Chiquimil Formation, indicates an age of  $6.68 \pm 0.02$  Ma (Marshall et al., 1979) and re-dated in  $7.14 \pm 0.02$  Ma (Latorre et al., 1997) near Puerta de Corral Quemado. Butler et al. (1984) suggested that the upper limit of the Chiquimil Formation was at 7.5 Ma.

We propose three alternatives for these discrepancies: i) The intruded red beds dated by Caelles et al. (1971) might correspond to the Hualfín Formation because this and the LAF are of similar lithology and very difficult to distinguish when they do not appear together (Bossi and Muruaga, 2009). ii) The LAF ends its sedimentation well before 6.73 Ma (the youngest age compatible with the magnetostratigraphic correlation). iii) A temporal variation from N to S for deposition of the sedimentary units or diachronism within the lower part of the Chiquimil Formation, since all the previous dates were calculated from samples at the Corral Quemado and Chiquimil/Entre Ríos localities, 75 and 125 km to the south of the Las Totoritas creek. We suggest a. This is reinforced with the variation in thickness of the units from N to S in the Santa María Valley. At the Las Totoritas creek Chiquimil Formation does not crop out, but in the Jujuil creek (south of the Santa María Valley) Ibañez (2001) reported a thickness of ~690 m. At that locality LAF has a thickness of just 340 m (Domínguez et al., 2013) and at Entre Ríos locality 215 m. All this is consistent with the original propositions by Reynolds et al. (1993) also proposed an important diachronism in the deposition of the continental Cenozoic units of the Andean foreland of NW Argentina. The recent dating of  $6.88 \pm 0.06$  Ma in the top of the LAF (Georgieff et al., 2014) reinforces this alternative.

Following these results we propose avoiding the term Santa María-Hualfín Basin as a unique unit due to different chronostratigraphic evolution and consequent diachronism within each depocenter.

## 7.3. Accumulation rates

Fig. 10 is a sediment accumulation rates plot constructed for the LAF with the interpreted ages of polarity reversals vs. the stratigraphic thickness. Several polarity reversals are found in the lower half of the studied sequence with a calculated average 0.19 mm/yr accumulation rate when the normal polarity zone at ~140 m is

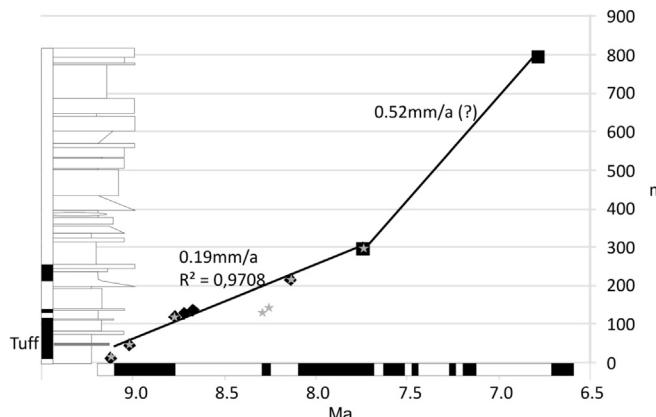


**Fig. 10.** Plot of age (with GPTS of Gradstein et al., 2012) vs. stratigraphic level (with the local magnetostratigraphic column) showing the sedimentation rate for Las Arcas Formation. The gray stars are a second alternative discussed in Sections 7.2 and 7.3.

correlated with cryptochron C4r.2r-1 (the same value is obtained when compared with the charts of Lourens et al., 2004; Cande and Kent, 1995 and Huestis and Acton, 1997). If the normal polarity zone at ~140 m is correlated with C4r.1n subchron 3 or 4 different accumulation rates are recorded (see gray stars in Fig. 10). The sedimentary Cenozoic units in the northern area of the Santa María Valley are called Payogastilla Group (Díaz and Malizia, 1983; Jordan and Alonso, 1987). The coeval unit within this Group to the LAF is the Palo Pintado Formation that contains 2 tuff levels that has been dated at  $10.29 \pm 0.11$  Ma (K/Ar) by Galli et al. (2008) and at  $5.27 \pm 0.28$  Ma ( $^{206}\text{Pb}/^{238}\text{U}$ ) by Coutand et al. (2006) and at  $5.98 \pm 0.32$  Ma by Bywater-Reyes et al. (2010), respectively. The unit comprises thickening and coarsening upward cycles, including matrix-supported conglomerates, fine to medium sandstones, and fine-grained sublithic sandstones that end in levels of green, brown and gray siltstones. Those deposits consist of transitional style wandering sand-gravel fluvial systems with small lakes (Galli et al., 2011; Galli and Reynolds, 2012; Galli et al., 2014). A magnetostratigraphic study of the Palo Pintado Formation (Galli et al., 2014) indicates sedimentation rates of 0.41 mm/yr until 8.8 Ma, 0.11 mm/yr from 8.8 Ma to 6.9 Ma and 0.66 mm/yr up to the top of the unit. If we compare the sedimentation rates of the Palo Pintado Formation (Galli et al., 2014) with the LAF calculated in this work they are very similar taken into account the first alternative of correlation.

Unfortunately, the upper half of the LAF shows exclusive reversed polarity. Assuming that this section was deposited until the end of the C3Ar chron (a dominant reversed period) a minimum 0.52 mm/yr average rate is computed (slightly different minimum rates of 0.55, 0.49 and 0.51 mm/yr if compared with the charts of Lourens et al., 2004; Cande and Kent, 1995 and Huestis and Acton, 1997). Butler et al. (1984) calculated an accumulation rate for the Chiquimil Formation of 0.56 mm/yr which is basically identical to that for the upper part of the LAF. Bossi et al. (2001) assume a sedimentation rate of 0.15–0.25 mm/yr for the top of LAF. Despite the fact that the accumulation rate of the upper part of LAF is actually not known, a major change in the rate of accumulation is evident after approximately 300 m of the succession. This coincides approximately with a minor change in the color of the strata and with a more conspicuous change in the grain size (coarsening upward and sandier beds). Villanueva García and Ovejero (1998, 1999) indicated an increase in the proportion of fragments of volcanic rocks from the middle of LAF upwards. The apparently sudden increase in the accumulation rate at around 7.7 Ma suggests a major

change in the subsidence rate of the basin and/or uplift of the source areas.

## 8. Conclusions

A magnetostratigraphic study was carried out in the Late Miocene Las Arcas Formation, exposed in the Santa María Valley, NW Argentina. The unit is composed of fine red sandstones and siltstones intercalated with some lenses of conglomerate typical of a fluvial setting. Detailed paleomagnetic processing of samples from 48 sites permitted determination of a pre-folding remanence in 26 sites. The mean remanence direction shows that this locality underwent non-significant rotation ( $11.0^\circ \pm 13.6^\circ$ ) since the Late Miocene. A reliable and precise isotopic date was obtained for the lower levels of the formation by  $^{40}\text{Ar}-^{39}\text{Ar}$  dating on volcanic amphiboles from a tuff intercalated ~45 m above the base of the unit yielding an age of  $9.01 \pm 0.12$  Ma. The local magnetic polarity column obtained from the paleomagnetic study correlated with the GPTS within the error limits in the age of the tuff and permitted to determine that the LAF was deposited from prior to 9.1 Ma up to not later than 6.8 Ma in the northern part of the Santa María Valley. The lower part of the unit was deposited during a stable tectonic period with a slow accumulation rate of fine sediments. At ~7.7 Ma a sudden increase in the tectonic activity produced a significant increase in the accumulation rate coinciding with an increment in the grain-size and a higher frequency of conglomerate sedimentation. This change likely reflects a tectonic reactivation and/or rise of the inversion velocity of the source area with the increase of sediment grain size.

## Acknowledgment

Superlnd 2000 (Torsvik et al., 2000) and Paleomagnetism Data Analysis v.4.2 (Enkin, 1994) software packages were used to analyze the paleomagnetics data. All laboratory analyses were conducted at the Laboratorio de Paleomagnetismo Daniel A. Valencia of the Instituto de Geociencias Básicas, Aplicadas y Ambientales de Buenos Aires (IGEBA), Departamento de Ciencias Geológicas de la Universidad de Buenos Aires (Argentina). This study was supported by Proyecto y Programas de Investigación: 26/G443 – 2 Secretaría de Ciencia y Técnica de la Universidad Nacional de Tucumán. CONICET (Argentine Research Council) is acknowledged for post-doctoral fellowships to C.M. Spagnuolo. Guillermo Ré is fully thanked for the help with the laboratory preparation of the samples and specimens. Constructive reviews by two anonymous reviewers and Regional Editor (Dr. Victor Ramos) significantly improved the final version.

## Appendix A. Supplementary data

Supplementary data related to this article can be found at <http://dx.doi.org/10.1016/j.jsames.2015.07.004>.

## References

- Acton, G., Guyodo, Y., Brachfeld, S., 2006. The nature of a cryptochron from a paleomagnetic study of chronC4r.2r recorded in sediments off the Antarctic Peninsula. *Phys. Earth Planet. Inter.* 156, 213–222.
- Arriagada, C., Roperch, P., Mpodozis, C., Fernández, R., 2006. Paleomagnetism and tectonics of the southern Atacama Desert region (25–28°S) Northern Chile. *Tectonics* 25, TC4001.
- Arriagada, C., Roperch, P., Mpodozis, C., Cobbold, P.R., 2008. Paleogene building of the Bolivian Oroocline: tectonic restoration of the central Andes in 2-D map view. *Tectonics* 27, TC6014.
- Aubry, L., Roperch, P., de Urreiztieta, M., Rossello, E., Chauvin, A., 1996. Paleomagnetic study along the south-eastern edge of the Altiplano-Puna Plateau: Neogene tectonic rotations. *J. Geophys. Res.* 101, 17.883–17.899.

- Beck Jr., M.E., 1988. Analysis of late Jurassic-recent paleomagnetic data from active plate margins of South America. *J. South Am. Earth Sci.* 1, 39–52.
- Beck, M.E., 1998. On the mechanism of crustal block rotations in the central Andes. *Tectonophysics* 299, 75–92.
- Besse, J., Courtillot, V., 2002. Apparent and true polar wander and the geometry of the geomagnetic field over the last 200 Myr. *J. Geophys. Res.* 107 (B11), 2300.
- Bossi, G.E., Palma, R., 1982. Reconsideración de la estratigrafía del Valle de Santa María, Provincia de Catamarca, Argentina. In: Congreso Latinoamericano de Geología, No. 5, Actas 1, pp. 155–172 (Buenos Aires).
- Bossi, G.E., Muruaga, C.M., 2009. Estratigrafía e inversión tectónica del 'rift' neógeno en el Campo del Arenal, Catamarca, NO Argentina. *Andean Geol.* 36 (2), 311–341.
- Bossi, G.E., Gavriloff, I., Esteban, G., 1998. Terciario. Estratigrafía, bioestratigrafía y paleogeografía. In: Gianfrancisco, M., Puchulu, M., Durango de Cabrera, J., Aceñolaza, G.F. (Eds.), *Geología de Tucumán. Colegio de Graduados Ciencias Geológicas de Tucumán*, second ed., pp. 87–110.
- Bossi, G.E., Georgieff, S.M., Gavriloff, I.J.C., Ibañez, L.M., Muruaga, C.M., 2001. Cenozoic evolution of the intramontane Santa María basin, Pampean Ranges, northwestern Argentina. *J. South Am. Earth Sci.* 14, 725–734.
- Butler, R.F., Marshall, L.G., Drake, R.E., Curtis, G.H., 1984. Magnetic polarity stratigraphy and K-Ar dating of late Miocene and early Pliocene continental deposits, Catamarca province, NW Argentina. *J. Geol.* 92, 623–636.
- Bywater-Reyes, S., Carrapa, B., Clementz, M., Schoenbohm, L., 2010. Effect of late Cenozoic aridification on sedimentation in the Eastern Cordillera of northwest Argentina (Angastaco basin). *Geology* 38, 235–238.
- Caelles, J.C., Clark, A.H., Farrar, E., McBride, S.L., Quirt, S., 1971. Potassium-argon ages of porphyry copper deposits and associated rocks in the Farallón Negro-Capillitas district, Catamarca, Argentina. *Econ. Geol.* 66, 961–964.
- Cande, S.C., Kent, D.V., 1992. A new geomagnetic polarity time scale for the Late Cretaceous and Cenozoic. *J. Geophys. Res.* 97 (B10).
- Cande, S.C., Kent, D.V., 1995. Revised calibration of the geomagnetic polarity timescale for the Late Cretaceous and Cenozoic. *J. Geophys. Res.* 100 (B4), 6093–6095.
- Coutand, I., Roperch, P., Chauvin, A., Cobbold, P.R., Gautier, P., 1999. Vertical-axis rotations across the Puna plateau (northwestern Argentina) from paleomagnetic analysis from Cretaceous and Cenozoic rocks. *J. Geophys. Res.* 104, 22965–22984.
- Coutand, I., Cobbold, P.R., de Urreiztieta, M., Gautier, P., Chauvin, A., Gapais, D., Rosello, E.A., López Gamundi, O., 2001. Style and history of Andean deformation, Puna plateau, northwestern Argentina. *Tectonics* 20 (2), 210–234.
- Coutand, I., Carrapa, B., Deenken, A., Schmitt, A.K., Sobel, E., Strecker, M.R., 2006. Orogenic plateau formation and lateral growth of compressional basins and ranges: insights from sandstone petrography and detrital apatite fission-track thermochronology in the Angastaco Basin, NW Argentina. *Basin Res.* 18, 1–26.
- de Urreiztieta, M., Gapais, D., Le Corre, C., Cobbold, P., Rosello, E., 1996. Cenozoic transgression and basin development at the southern edge of the Puna plateau, NW Argentina. *Tectonophysics* 254, 17–39.
- Díaz, I.J., Malizia, D.C., 1983. Estudio geológico y sedimentológico del Terciario superior del Valle Calchaquí (Dept. San Carlos, provincia de Salta). *Bol. Sedimentol.* 2 (1), 8–21.
- Domínguez, L.I., Spagnuolo, C.M., Georgieff, S.M., Ibañez, L.M., 2013. Paleomagnetic study of the Late Miocene Las Arcas Formation, Pampean Ranges, Northwestern Argentina. *Latinmag Lett.* 3 (PB05), 1–5. October 2013–Volume 3–Number 3.
- Enkin, R.J., 1994. A Computer Program Package for Analysis and Presentation of Paleomagnetic Data, vol. 16. Pacific Geoscience Centre. Geological Survey of Canada, Sidney, Canada.
- Enkin, R.J., 2003. The direction-correction tilt test: an all-purpose tilt/fold test for palaeomagnetic studies. *Earth Planet. Sci. Lett.* 212, 151–166.
- Galli, C.I., Ramírez, A., Barrientos, C., Reynolds, J., Viramonte, J.G., Idleman, B., 2008. Estudio de proveniencia de los depósitos del Grupo Payogastilla (Mioceno Medio-Superior) aflorantes en el río Calchaquí, provincia de Salta, Argentina. In: 17º Congreso Geológico Argentino, Actas 1, pp. 353–354 (San Salvador de Jujuy).
- Galli, C.I., Anzotegui, L.M., Horn, Y., Morton, S., 2011. Paleoambiente y Paleocomunidades de la Formación Palo Pintado (Mioceno-Plioceno), provincia de Salta, Argentina. *Rev. Mex. Cienc. Geol.* 28, 161–174.
- Galli, C.I., Reynolds, J., 2012. Evolución paleoambiental del Grupo Payogastilla (Eoceno- Plioceno) en el valle Calchaquí-Tonco, provincia de Salta, Argentina. In: 13º Reunión Argentina de Sedimentología, Relatorio, pp. 67–80 (Salta).
- Galli, C.I., Coira, B., Alonso, R., Reynolds, J., Matteini, M., Hauser, N., 2014. Tectonic controls of the evolution of the Andean Cenozoic foreland basin: evidence from fluvial system variations in the Payogastilla Group, in the Calchaquí, Tonco and Ambalayo Valleys, NW Argentina. *South Am. Earth Sci.* 52, 234–259.
- Galván, A.F., Ruiz Huidobro, O., 1965. Geología del valle de Santa María. Estratigrafía de las Formaciones Mesozoico-Terciarias. *Acta Geol. Lilloana* 7, 217–230.
- Georgieff, S.M., 1996. Cuencas de antepaís: una revisión. Evolución tectosedimentaria en el Terciario-Cuaternario del Valle de Santa María, Tucumán y Catamarca, Argentina. In: XIII Congreso Geológico Argentino y III Congreso de Exploración de Hidrocarburos, 2, pp. 161–170 (Buenos Aires).
- Georgieff, S.M., 1998. Análisis paleoambiental de la porción inferior de la Formación Andaluhalua en la zona central del valle de Santa María, Tucumán y Catamarca, Argentina. Universidad Nacional de Tucumán (PhD thesis).
- Georgieff, S.M., Díaz, A., 2014. Modelo paleoambiental de la Formación Las Arcas (Mioceno Superior), quebrada del Mal Paso, Valles Calchaquíes del sur de Salta. In: 14º Reunión Argentina de Sedimentología: 114. Puerto Madryn, Chubut.
- Georgieff, S.M., Ibañez, L.M., Vides, M.E., Anis, K.B., Nieva, S.M., 2014. Paleógeno y Neógeno de Tucumán: Estratigrafía y paleoambientes sedimentarios. In: Moyano, M.S., Puchulu, M.E., Fernández, D.S., Vides, M.E., Nieva, S., Aceñolaza, G. (Eds.), *Geología de Tucumán. Publ. Esp. Colegio de Graduados de Ciencias Geológicas de Tucumán*, pp. 106–123.
- González Bonorino, F., 1950. Algunos problemas geológicos de las Sierras Pampeanas. *Rev. la Asoc. Geol. Argent.* 5 (3), 81–110.
- Gradstein, F.M., Ogg, J.G., Smith, A.G. (Eds.), 2004. In: *A Geologic Time Scale 2004*. Cambridge University Press, Cambridge, UK.
- Gradstein, F.M., Ogg, J.G., Schmitz, M.D., Ogg, G.M. (Eds.), 2012. *The Geologic Time Scale 2012* (Elsevier).
- Halter, W.E., Bain, N., Becker, K., Heinrich, C.A., Landtwing, M., VonQuadt, A., Clark, A.H., Sasso, A.M., Bissig, T., Tosdal, R.M., 2004. From andesitic volcanism to the formation of a porphyry Cu-Au mineralizing magma chamber: the Farallón Negro Volcanic Complex, northwestern Argentina. *J. Volcanol. Geotherm. Res.* 136, 1–30.
- Homke, S., Vergés, J., Garcés, M., Emami, H., Karpuz, R., 2004. Magnetostratigraphy of Miocene–Pliocene Zagros foreland deposits in the front of the Push-e Kush Arc (Lurestan Province, Iran). *Earth Planet. Sci. Lett.* 225, 397–410.
- Huestis, S.P., Acton, G.D., 1997. On the construction of geomagnetic timescales from non-prejudicial treatment of magnetic anomaly data from multiple ridges. *Geophys. J. Int.* 129, 176–182.
- Ibañez, L.M., 2001. Análisis paleoambiental de la Formación Chiquimil en el valle de Santa María. Salta, Tucumán y Catamarca. Universidad Nacional de Tucumán (PhD thesis).
- Irigoyen, M.V., Buchan, K.L., Brown, R.L., 2000. Magnetostratigraphy of Neogene Andean foreland-basin strata, lat 33° S, Mendoza Province, Argentina. *Geol. Soc. Am. Bull.* 112, 803–816.
- Japas, M.S., Ré, G.H., 2006. Margin Curvature Related to Subduction of Oblique Aseismic Ridges. In: *Backbone of the Americas-Patagonia to Alaska*. Paper N°3-2. Mendoza.
- Japas, M.S., Ré, G.H., 2012. Neogene tectonic block rotations and margin curvature at the Pampean flat slab segment (28°–33° SL, Argentina). *Geoacta* 37 (1), 1–4.
- Johnson, P.A., Jordan, T.E., Johnson, N.M., Naeser, C.W., 1986. Magnetic polarity stratigraphy, age and tectonic setting of foreland basin, San Juan province, Argentina. *Int. Assoc. Sedimentol. Spec. Publ.* 8, 63–75.
- Jordan, T.E., Alonso, R., 1987. Cenozoic stratigraphy and basin tectonics of the Andes Mountains, 20°–28° South latitude. *Am. Assoc. Pet. Geol. Bull.* 71 (1), 49–64.
- Jordan, T.E., Rutty, P.M., McRae, L.E., Beer, J.A., Tabbutt, K.D., 1990. Magnetic polarity chronostratigraphy of the Miocene Rio Azul section, Precordillera thrust belt, San Juan Province, Argentina. *J. Geol.* 98, 519–539.
- Jordan, T.E., Allmendinger, R.W., Damanti, J.F., Drake, R.E., 1993. Chronology of motion in a complete thrust belt: the Precordillera, 30°–31° S, Andes Mountains. *J. Geol.* 101, 137–158.
- Kay, S.M., Mpodozis, C., 2002. Magmatism as a probe to the Neogene shallowing of the Nazca plate beneath the modern Chilean flat slab. *J. S. Am. Earth Sci.* 15, 39–57.
- Kirschvink, J.L., 1980. The least squares line and plane and the analysis of paleomagnetic data. *Geophys. J. Roy. Astron. Soc.* 62, 699–718.
- Latorre, C., Quade, J., McIntosh, W.C., 1997. The expansion of the C4 grasses and global change in the Late Miocene: stable isotope evidence from the Americas. *Earth Planet. Sci. Lett.* 146, 83–96.
- Lourens, L.J., Hilgen, F.J., Laskar, J., Shackleton, N.J., Wilson, D., 2004. In: Gradstein, F., Ogg, J. et al. (Eds.), *A Geologic Time Scale*. Cambridge University Press, United Kingdom, pp. 409–440.
- Malizia, D.C., Reynolds, J.H., Tabutt, K.D., 1995. Chronology of Neogene sedimentation, stratigraphy, and tectonism in the Campo de Talampaya region, La Rioja province, Argentina. *Sediment. Geol.* 96, 231–255.
- Marrett, R., Strecker, M., 2000. Response of intracontinental deformation in the central Andes to late Cenozoic reorganization of South American Plate motions. *Tectonics* 19, 452–467.
- Marshall, L.G., Patterson, B., 1981. Geology and Geochronology of the Mammal-Bearing Tertiary of the Valle de Santa María and Río Corral Quemado, Catamarca Province, Argentina. *FIELDIANA. Geol. New Ser.* 9, 1–78.
- Marshall, L.G., Butler, R.F., Drake, R.E., Curtis, G.H., Tedford, R.H., 1979. Calibration of the Great American Interchange. *Science* 204, 272–279.
- Matuyama, M., 1929. On the direction of magnetization of basalt in Japan, Tysoen and Manchuria. *Proc. Jpn. Acad.* 5, 203–205.
- McFadden, P.L., Lowes, F.J., 1981. The discrimination of mean directions drawn from Fisher distributions. *Geophys. J. R. Astron. Soc.* 67, 19–33.
- McFadden, P.L., McElhinny, M.W., 1990. Classification of the reversal test in paleomagnetism. *Geophys. J. Int.* 103, 725–729.
- Mon, R., 1976. La tectónica del borde oriental de los Andes, en las provincias de Salta, Tucumán y Catamarca, República Argentina. *Rev. Asoc. Geol. Argent.* 31 (2), 65–72.
- Mon, R., 1979. Esquema tectónico de los Andes del norte argentino. *Rev. la Asoc. Geol. Argent.* 34, 70–76.
- Mortimer, E., Carrapa, B., Coutand, I., Schoenbohm, L., Sobel, E., Sosa Gómez, J., Strecker, M., 2007. Fragmentation of a foreland basin in response to out-of-sequence basement uplifts and structural reactivation: El Cajón–Campo del Arenal basin, NW Argentina. *GSA Bull.* 119 (5/6), 637–653.
- Opdyke, N.D., Channell, J.E.T., 1996. *Magnetic Stratigraphy*. Academic press, San Diego, CA, 346 pp.

- Peirano, A., 1956. Observaciones generales sobre la tectónica y los depósitos terciarios del cuadrángulo 26 S-64 30°, 0-28 30°S-67 O en el noroeste argentino. *Acta Geol. Lilloana* 1, 61–144.
- Prezzi, C., Caffé, P., Somoza, R., 2004. New paleomagnetic data from the northern Puna and western Cordillera Oriental, Argentina: a new insight on the timing of rotational deformation. *J. Geodyn.* 38, 93–115.
- Ramos, V.A., 1999. Rasgos estructurales del territorio argentino. 1. Evolución tectónica de la Argentina. In: Caminos, R. (Ed.), *Geología Argentina*. Instituto de Geología y Recursos Minerales, Anales, vol. 29(24), pp. 715–784 (Buenos Aires).
- Randall, D., 1998. A new Jurassic-recent apparent polar wander path for South America and a review of central Andean tectonic models. *Tectonophysics* 299, 49–74.
- Ré, G.H., 2008. Magnetoestratigrafías del NO argentino (entre 27° y 31° S) aplicadas al análisis de la deformación andina, y su relación con la subducción de la placa de Nazca durante el Cenozoico tardío. Universidad de Buenos Aires (PhD thesis).
- Ré, G.H., Japas, M.S., Barredo, S.P., 2001. Análisis de fábrica deformacional (AFD): el concepto fractal cualitativo aplicado a la definición de lineamientos cinemáticos neógenos en el Noroeste Argentino. In: Asociación Geológica Argentina, Serie D: Publicación Especial 5: 75–82. 10<sup>th</sup> Reunión sobre Microtectónica. Buenos Aires.
- Reynolds, J.H., Jordan, T.E., Johnson, N.M., Damanti, J.F., Tabbutt, K.D., 1990. Neogene deformation of the flat-slab subduction segment of the Argentine-Chilean Andes: magnetostratigraphic constraints from Las Juntas, La Rioja province, Argentina. *Geol. Soc. Am. Bull.* 102, 1607–1622.
- Reynolds, J.H., Hernández, R., Naeser, C.W., Hernández, R., 1993. Geological Society of America Abstracts with Programs (Boston, MA). Chronostratigraphic Calibration of Neogene Sedimentation in the Argentine Subandes, Salta Province, Northern Argentina, vol. 25(6), p. A-473.
- Reynolds, J.H., Hernández, R., Galli, C., Idelman, B., 2001. Magnetostratigraphy of the Quebrada La Porcelana section, Sierra de Ramos, Salta province, Argentina. Initial age limits on the regional Neogene lithostratigraphy and uplift of the southern Sierras Subandinas. *J. South Am. Earth Sci.* 14, 681–692.
- Ruiz Huidobro, O.J., 1960. El Horizonte Calcáreo – Dolomítico en la Provincia de Tucumán. *Acta Geol. Lilloana* 3, 147–171.
- Ruiz Huidobro, O., 1966. Contribución a la geología de las Cumbres Calchaquíes y Sierra del Aconquija (Tucumán–Catamarca). *Acta Geol. Lilloana* 8, 215.
- Sobel, E.R., Strecker, M.R., 2003. Uplift, exhumation and precipitation: tectonic and climatic control of Late Cenozoic landscape evolution in the northern Sierras Pampeanas, Argentina. *Basin Res.* 15, 431–451.
- Somoza, R., Tomlinson, A., 2002. Paleomagnetism in the Precordillera of northern Chile (22°–30°S): implications for the history of tectonic rotations in the Central Andes. *Earth Planet. Sci. Lett.* 194, 369–381.
- Somoza, R., Singer, S., Coira, B., 1996. Paleomagnetism of upper Miocene ignimbrites at the Puna: an analysis of vertical-axis rotations in the Central Andes. *J. Geophys. Res.* 101, 11387–11400.
- Sosa Gómez, J., Georgieff, S.M., Díaz, A., 2014. Compartimentalización de las cuencas intermontanas de las Sierras Pampeanas Noroccidentales: controles sobre los depocentros neógenos de los Valles Calchaquíes del sur de Salta y oeste de Tucumán. In: 14<sup>th</sup> Reunión Argentina de Sedimentología, pp. 259–260 (Puerto Madryn, Chubut).
- Spagnuolo, C.M., Rapalini, A.E., Astini, R.A., 2008. Palaeomagnetic confirmation of Palaeozoic clockwise rotation of the Famatina ranges (NW Argentina): implications for the evolution of the SW margin of Gondwana. *Geophys. J. Int.* 173 (1), 63–78.
- Spagnuolo, C.M., Rapalini, A.E., Astini, R.A., 2010. Reinterpretation of the Ordovician rotations in NW Argentina and Northern Chile: a consequence of the Pre-cordillera collision? *Int. J. Earth Sci. (Geol. Rundsch.)* 100, 603–618.
- Strecker, M., 1987. Late Cenozoic Landscape Development. The Santa María Valley, Northwestern Argentina. Cornell University, Ithaca, NY (Ph.D. thesis).
- Sun, Z., Yang, Z., Pei, J., Ge, X., Wang, X., Yang, T., Li, W., Yuan, S., 2005. Magnetostratigraphy of Paleogene sediments from northern Qaidam Basin, China: implications for tectonic uplift and block rotation in northern Tibetan plateau. *Earth Planet. Sci. Lett.* 237, 635–646.
- Taylor, G.K., Grocott, J., Pope, A., Randall, D.E., 1998. Mesozoic fault systems, deformation and fault block rotation in the Andean forearc: a crustal scale strike-slip duplex in the Coastal Cordillera of northern Chile. *Tectonophysics* 299, 93–109.
- Taylor, G.K., Dashwood, B., Grocott, J., 2005. The central Andean rotation pattern: evidence of an anomalous terrane in the forearc of northern Chile from paleomagnetic rotations. *Geology* 33, 777–780.
- Torsvik, T.H., Briden, J.C., Smethurst, M.A., 2000. IAPD2000. NGU, Free Software.
- Toselli, J.A., Rossi, J.N., 1998. El basamento metamórfico-igneo de las Sierras Pampeanas de la Provincia de Tucumán. In: Gianfrancisco, M., Puchulu, M.E., Durango de Cabrera, J., Aceñolaza, G.F. (Eds.), *Geología de Tucumán. Colegio de Graduados en Ciencias Geológicas de Tucumán*, pp. 47–56.
- Toselli, J.A., López, J.P., Sardi, F.G., 1999. El basamento metamórfico en Cumbres Calchaquíes noroccidentales, Aconquija, Ambato y Ancasti: Sierras Pampeanas. In: González Bonorino, G., Omarini, R., Viramonte, J. (Eds.), *Relatorio XIV Congreso Geológico Argentino. Geología del Noroeste Argentino*, vol. 1, pp. 73–79.
- Villanueva García, A., Ovejero, R., 1998. Procedencia de las areniscas de las formaciones San José y Las Arcas (Neógeno) en la localidad de Entre Ríos, Catamarca. *Rev. Asoc. Geol. Argent.* 53, 158–166.
- Villanueva García, A., Ovejero, R., 1999. Petrografía de las unidades basales del Grupo Santa María (Neógeno), en los Andes Centrales (26°–27°S, 66°W), Noroeste Argentino. *XIV Congr. Geol. Argent.* 1, 76.
- Vizán, H., Geuna, S., Melchor, R., Bellosi, E.S., Lagorio, S.L., Vásquez, C., Japas, M.S., Ré, G., Do Campo, M., 2013. Geological setting and paleomagnetism of the Eocene red beds of Laguna Brava Formation (Quebrada Santo Domingo), northwestern Argentina. *Tectonophysics* 583, 105–123.
- Watson, G., Enkin, R., 1993. The fold test in paleomagnetism as a parameter estimation problem. *Geophys. Res. Lett.* 20 (19), 2135–2137.
- Zambrano, O., Rapalini, A.E., Dávila, F.M., Astini, R.A., Spagnuolo, C.M., 2010. Magnetostratigraphy and paleomagnetism of early and middle Miocene synorogenic strata: basement partitioning and minor block rotation in the Argentine broken foreland. *Int. J. Earth Sci.* 100 (2–3), 591–602.